METALLURGY OF NON-FERROUS METALS / МЕТАЛЛУРГИЯ ЦВЕТНЫХ МЕТАЛЛОВ

UDC 621.365.2 : 669.2/8
https://doi.org/10.17073/0021-3438-2023-1-26-38

Research article
Научная статья

Investigation of Pobeda furnace bubbling zone physics using cold modeling method

Part 3. The hydro-gas dynamics of combined blowing of liquid by gas using bottom and lateral lances

K.V. Bulatov[1], **V.P. Zhukov**[1], **E.V. Bratygin**[1], **N.A. Tomilov**[1], **V.A. Menshchikov**[2]

[1] **JSC "Ural Research and Design Institute of Mining Processing, Metallurgy, Chemistry, Standartization"**
87 Khokhryakova str., Ekaterinburg, 620063, Russia

[2] **Ural Federal University n.a. the First President of Russia B.N. Eltsin**
17 Mira str., Ekaterinburg, 620002, Russia

✉ Vladimir P. Zhukov (zhukov.v.p@mail.ru)

Abstract: Hydro-gas regularities of liquid combined blowing by gas were studied using cold modeling method at Archimedes criterion for lateral Ar_l = 12÷120 and bottom blowing Ar_b = 5÷60 simulating Pobeda bubbling unit. The blowing was performed simultaneously by bottom lance vertically fixed in centre of reactor and by the lateral lance which was attached at an angle 5° to the horizontal axis. The quantitative estimation of instantaneous and average circulation velocities (V_{av}) of liquid flow elements in different bath areas, depending on the location of blowing zone and Archimedes criterion, was performed. The liquid motion trajectory was determined. A vortex zone was revealed near the liquid surface and the reactor shell, where instantaneous velocity of the liquid flow elements changes from 69.9 to 181.1 mm/s and V_{av} = 123.8 mm/s. The circulation flows fade in the bulk of liquid and V_{av} decreases from 123.8 to 47.0 and 54.1 mm/s. It was shown that, in general, circulation velocity depends on the blowing intensity and appears to be higher for the zone of overlapping of lateral and bottom streams. The dynamic blowing conditions, which ensure the direct contact of lateral and bottom jets leading to their interflow and increased spatter formation, were identified. The characteristics of 3 types of surface oscillations for interface phases "pure liquid – gas-liquid layer", as well as the estimation of the lateral and bottom blowing impact on the type of oscillation were provided. It has been noted that the introduction of the bottom blowing (Ar_b = 5) causes the wave-like motion of liquid (the 2nd type) along with the transverse oscillations of the 1st type, and at higher values of Ar_b = 25 the angular oscillations of the 3rd type develop. It has been shown that the presence of a lateral jet at the combined blowing decreases angles of bath swinging to 8–12° to horizontal axis. For the estimation of oscillation intensity, $\Delta h_l = (h_l)_{max} - (h_l)_{min}$ value, which means the difference between maximum $(h_l)_{max}$ and minimum $(h_l)_{min}$ height of liquid for the full-wave oscillations (τ), was introduced. The height of liquid (h_l) was plotted as a function of τ, Ar_l, Ar_b, Δh_l was determined on the basis of obtained graph values, which varied upon modeling over the range of 7.7–69.5 mm. The relation between the liquid circulation velocity and the oscillation value (Δh_l) was established for different bath zones and dynamic conditions of the blowing. The impact of all oscillations types on potential erosive lining wear of Pobeda bubbling unit and the completeness of adoption of charging material nearby the bath surface was investigated.

Keywords: combined blowing, lateral lance, bottom lance, Archimedes criterion, Pobeda melting unit, liquid circulation, instantaneous circulation velocity, average circulation velocity, blowing zone, coordinate, interphase oscillation

For citation: Bulatov K.V., Zhukov V.P., Bratygin E.V., Tomilov N.A., Menshchikov V.A. Investigation of Pobeda furnace bubbling zone physics using cold modeling method. Part 3. The hydro-gas dynamics of combined blowing of liquid by gas using bottom and lateral lances. *Izvestiya. Non-Ferrous Metallurgy*. 2023; 29 (1): 26–38. (In Russ.). https://doi.org/10.17073/0021-3438-2023-1-26-38

Исследование физических явлений в барботажной зоне плавильного агрегата «Победа» методом холодного моделирования

Сообщение 3. Гидрогазодинамика комбинированной продувки жидкости газом с помощью донной и боковой фурм

К.В. Булатов[1], **В.П. Жуков**[1], **Е.В. Братыгин**[1], **Н.А. Томилов**[1], **В.А. Меньщиков**[2]

[1] **ОАО «Уральский научно-исследовательский и проектный институт горного дела, обогащения, металлургии, химии, стандартизации» (ОАО «Уралмеханобр»)**
620063, Россия, г. Екатеринбург, ул. Хохрякова, 87

[2] **Уральский федеральный университет им. первого Президента России Б.Н. Ельцина**
620002, Россия, г. Екатеринбург, ул. Мира, 17

✉ Владимир Петрович Жуков (zhukov.v.p@mail.ru)

Аннотация: Методом холодного моделирования в интервалах величин критерия Архимеда для бокового ($Ar_б$ = 12÷120) и донного ($Ar_д$ = 5÷60) дутья применительно к условиям работы барботажного плавильного агрегата «Победа» (ПАП) исследованы гидрогазодинамические закономерности комбинированной продувки жидкости газом. Продувку осуществляли одновременно донной фурмой, установленной вертикально по центру реактора, и боковой, расположенной под углом 5° к горизонтальной оси. Проведена количественная оценка мгновенной и средней ($V_{ср}$) скоростей циркуляции элементов потока жидкости на разных участках ванны в зависимости от местонахождения зоны продувки и критериев Архимеда. Определена траектория движения жидкости. Вблизи поверхности жидкости и корпуса реактора обнаружена вихревая зона, где мгновенная скорость движения элемента потока жидкости изменяется от 69,9 до 183,1 мм/с и $V_{ср}$ = 123,8 мм/с. В объеме жидкости циркуляционные потоки затухают, и $V_{ср}$ уменьшается от 123,8 до 47,0 и 54,1 мм/с. Показано, что в общем случае скорость циркуляции зависит от интенсивности продувки на фурмах и становится выше для области наложения боковой и донной струй. Определены динамические условия продувки, обеспечивающие непосредственный контакт бокового и донного факелов, приводящий к слиянию потоков и повышенному брызгообразованию. Приведена характеристика 3 видов колебаний поверхности раздела фаз «чистая жидкость – газожидкостный слой» и дана оценка влияния бокового и донного дутья на разновидность возникающих колебаний. Отмечено, что ввод донного дутья ($Ar_д$ = 5) приводит, наряду с поперечными колебаниями 1-го типа, к появлению волнообразного движения жидкости (2-й тип), а при более высоких значениях $Ar_д$ = 25 – к угловым колебаниям (3-й тип). Показано, что при комбинированной продувке наличие бокового факела уменьшает углы раскачивания ванны к горизонту до 8–12°. Для оценки интенсивности колебаний введена величина $\Delta h_ж = (h_ж)_{max} - (h_ж)_{min}$, т.е. разность между максимальной $(h_ж)_{max}$ и минимальной $(h_ж)_{min}$ высотой жидкости за полный цикл колебаний (τ). Построены зависимости высоты жидкости ($h_ж$) от τ, $Ar_б$ и $Ar_д$, на основании которых определены величины $\Delta h_ж$, варьируемые при моделировании в интервале 7,7–69,5 мм. Для различных областей ванны и динамических условий продувки установлена взаимосвязь между скоростью циркуляции жидкости и величиной колебаний ($\Delta h_ж$). Рассмотрено влияние всех видов колебаний на возможный эрозивный износ футеровки ПАП и полноту усвоения шихтовых материалов вблизи поверхности ванны.

Ключевые слова: комбинированная продувка, боковая фурма, донная фурма, критерий Архимеда, плавильный агрегат «Победа», циркуляция жидкости, мгновенная скорость циркуляции, средняя скорость циркуляции, область продувки, координаты, колебания границы раздела фаз

Для цитирования: Булатов К.В., Жуков В.П., Братыгин Е.В., Томилов Н.А., Меньщиков В.А. Исследование физических явлений в барботажной зоне плавильного агрегата «Победа» методом холодного моделирования. Сообщение 3. Гидрогазодинамика комбинированной продувки жидкости газом с помощью донной и боковой фурм. *Известия вузов. Цветная металлургия*. 2023; 29 (1): 26–38. (In Russ.). https://doi.org/10.17073/0021-3438-2023-1-26-38

Introduction

Previously, the hydrodynamic patterns of separate (lateral and bottom) liquid blowing using a single lance in a gas envelope were studied [1—3]. This paper is aimed at estimating the physics upon the combined outflow of gas into the liquid through the lateral and bottom nozzles. Due to being split, the combined blowing allows to integrally impact the melt with several jets and to influence the physicochemical regularities of metallurgical reactions, respectively.

Currently, the majority of publications are devoted to autogenous processes, addressing the operation of units with a submersible vertical lance, as well as various combinations of bottom or lateral blowing with top blowing in relation to steelmaking technology [4—21]. At the same time, each combination of blowing devices is characterized by optimal geometric and gas-dynamic parameters. In addition, it is known that the melting productivity of copper sulfide concentrate in Pobeda melting unit (PMU) depends on the ratio of bottom and lateral blowing costs [5]. The geometry of the mutual arrangement of the lances and the direction of the streams in the melt have different effects on the intensity of the bath mixing. The mathematical description of hydro-gas-dynamics as applied to bubbling conditions and the solution of a complete system of differential equations for calculating the true velocity of currents in two and three directions are of significant difficulty. Therefore, the melt circulation velocity was determined experimentally using the cold modeling method.

Experimental methods

The experiments were carried out using lateral and bottom lances installed in the reactor of the laboratory plant as used in previous papers [1—3]. The location of the lances in relation to the axes of the nozzles and the reactor is shown in Fig. 1. The bottom lance *1* was vertically fixed in the center of the reactor, and the lateral lance *2* was attached at an angle of $\alpha = 5°$ to the horizontal axis. The lances were placed in the same plane of the cross section of the plant at a distance of $h = 42$ mm between the centers of the tips of the lateral and bottom lances. During the modeling, the change in the coordinates of the location of individual particles-indicators *3* in current blowing time τ_i was monitored, the streamlines were drawn, and the liquid circulation velocity was calculated.

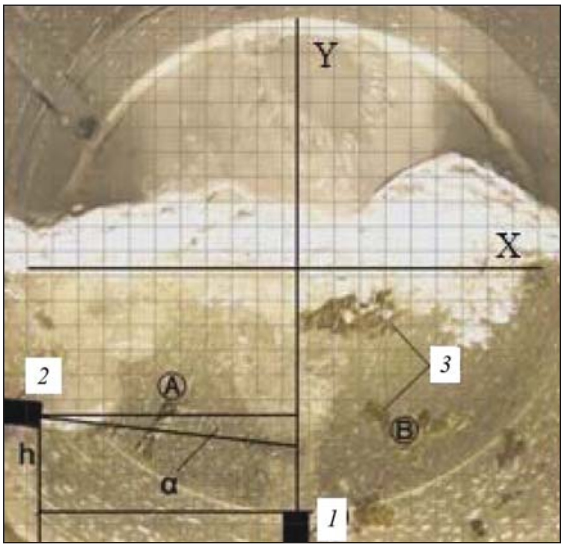

Fig. 1. The position of lance in relation to the axes of the cross-section of the reactor with a conditional coordinate grid

Рис. 1. Положение фурм относительно осей поперечного сечения реактора с условной координатной сеткой

The object of research was the hydrodynamics between the lateral and bottom streams in the conditional area *A* and beyond the bottom stream in area *B*. During the data processing, the film fragments allowing to visualize the sequential movement of a specific indicator within the field of the investigated areas of the bath were used. The total distance (S) of the curved path of the indicator was assumed to be the sum of the absolute values of the lengths of the segments (S_i) by which its center moves at each ith point of n images:

$$S = \sum_{i=1}^{n} \left| S_i \right|. \quad (1)$$

In the Cartesian coordinate system, the distance between points is as follows:

$$S_i = \sqrt{(x_{i+1} - x_i)^2 + (y_{i+1} - y_i)^2}, \quad (2)$$

where i stands for the number of the image in the series; x_i, y_i are the indicator coordinates in the ith image; x_{i+1}, y_{i+1} are the coordinates in the next image within the following time: $\Delta\tau = \tau_{i+1} - \tau_i$.

Instantaneous (V_i) and average (V_{av}) values of indicator movement velocity were calculated by the following equations:

$$V_i = S_i / \Delta\tau, \quad (3)$$

$$V_{av} = S/(n\Delta\tau), \quad (4)$$

where $\Delta\tau$ stands for the time interval between the shots, which is equal to 0.143 s according to the conditions of the experiment.

The example shown in Fig. 2 illustrates the methodology for determining the trajectory and calculating the values of V_i, V_{av} for the movement of the indicator mark in the liquid between the lateral and bottom streams when analyzing 6 fragments of the film record depicted in Fig. 3. In the coordinate system (Fig. 2), the horizontal axis X is directed along the bottom nozzle section, while the vertical axis Y passes through its

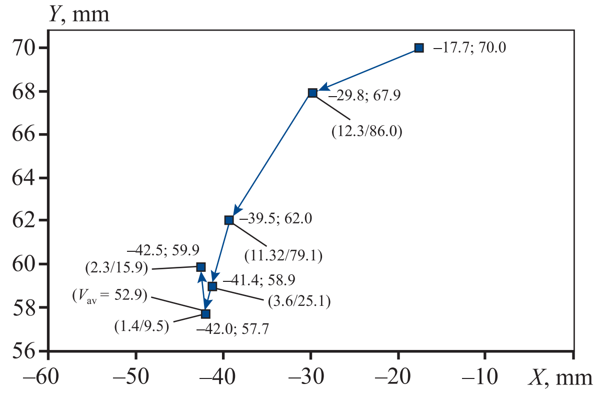

Fig. 2. The current coordinates and the trajectory of the indicator movement in $\Delta\tau = 0.143$ s

In brackets the numerator is the length of the segment (S_i, mm), the denominator is the instantaneous velocity (V_i, mm/s)

Рис. 2. Текущие кординаты и траектория перемещения индикатора через $\Delta\tau = 0{,}143$ с

В скобках числитель – длина отрезка (S_i, мм), знаменатель – мгновенная скорость (V_i, мм/с)

center. A two-dimensional section of the bath with a symmetry plane in the middle of the section is considered, assuming that the mixing conditions in other sections do not affect this velocity field. The current location of the particles was also determined using Paint.net software [1]. When comparing the coordinates in the image measurement system with real coordinates, the position of the axes and the scale of the image were taken into account.

The motion of liquid in the blowing area occurs due to the translational energy of the gas stream, which is determined by the magnitude of its momentum. When using a shell lance, the total momentum of motion (i_t) translated to the liquid by annular (i_{sh}) and circular (i_c) streams is equal to the sum of these values as per the principle of conservation of moment [6]:

$$i_t = i_{sh} + i_c. \qquad (5)$$

According to the experimental conditions [1], the cross-sectional areas of the annular (f_{sh}) and circular (f_c) nozzles are equal, therefore, the equivalent size of the annular nozzle is as follows: $d_e = (4f_{sh}/\pi)^{1/2}$, and $d_e = d_{sh} = d_c$. As the momentum of the stream is generally determined by the following equation:

$$i = \rho_g \omega_g^2 f_n, \qquad (6)$$

where ρ_g stands for gas density, kg/m^3, ω_g stands for the velocity of gas outflow from the nozzle, m/s, and f_n stands for the cross-sectional area of the nozzle, m^2, and the Archimedes criterion is determined under the following equation:

$$\mathrm{Ar} = \frac{\rho_g \omega_g^2}{\rho_l g d_n}, \qquad (7)$$

where d_n stands for the nozzle diameter, m, we obtain the following expression, taking into account expression (5):

$$\mathrm{Ar}_t = \mathrm{Ar}_{sh} + \mathrm{Ar}_c, \qquad (8)$$

where Ar_t stands for total Archimedes criterion; Ar_{sh}, Ar_c stand for its values of gas outflow from the shell and the central nozzle, respectively.

The additive nature of equations (5), (8) indicates the possibility of modeling of physics in the investigated areas of the bath using only one cylindrical nozzle for blowing with gas supply at a value of Ar_t equivalent to the values of Ar_{sh}, Ar_c.

The liquid was treated by the lateral and bottom streams at a blowing flow rate through a circular nozzle corresponding to $\mathrm{Ar}_l = 12 \div 120$ and $\mathrm{Ar}_b = 5 \div 60$ Archimedes criteria for the lateral and bottom gas injection. The latter are in the range of Ar_t values of equation (8) and correspond to the dynamic conditions of the previously performed cold molding with separate gas supply to the annulus and the central cavity of the lance [1—3].

Modeling results and discussion

Fig. 4 represents a diagram of motion of the liquid in the laboratory reactor with an inner radius $R = 135$ mm,

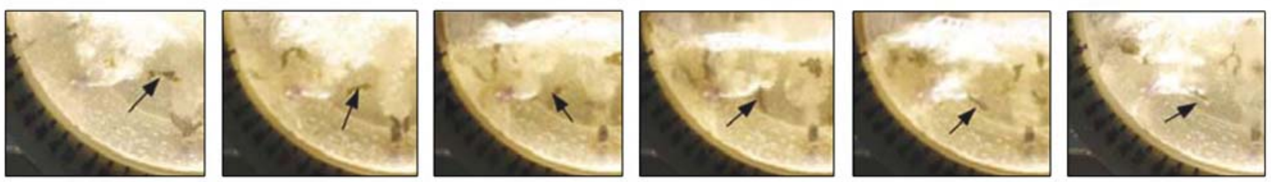

Fig. 3. The film record of the indicator successive movement (marked by the arrow) in the bubbling area (A) with the interval of $\Delta\tau = 0.143$ s

Рис. 3. Кинограмма последовательного движения индикатора (указан стрелкой) в области барботажа (A) с шагом $\Delta\tau = 0{,}143$ с

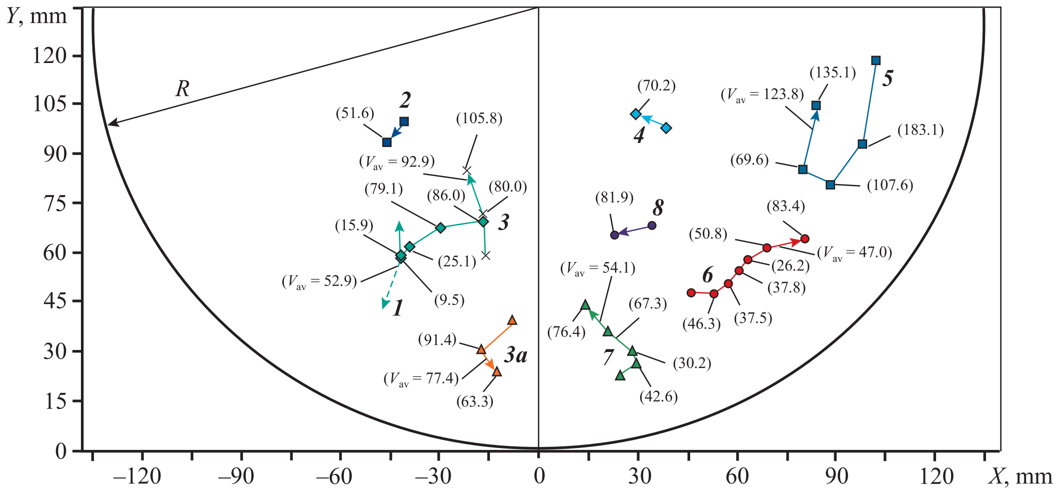

Fig. 4. The scheme of liquid motion and velocity field depending on the blowing conditions and the coordinates of the bubbling area

For combined lateral and bottom blowing – curves ***1***, ***4***, ***6–8*** ($Ar_l = Ar_b = 25$) and ***3*** ($Ar_l = 25$, $Ar_b = 5$); ***3a*** – separate lateral blowing ($Ar_l = 25$); ***2***, ***5*** – only bottom blowing ($Ar_b = 25$)

Рис. 4. Схема движения жидкости и поле скоростей в зависимости от условий продувки и координат области барботажа

Для совместного бокового и донного дутья – кривые ***1***, ***4***, ***6–8*** ($Ar_б = Ar_д = 25$) и ***3*** ($Ar_б = 25$, $Ar_д = 5$); ***3a*** – отдельная боковая продувка ($Ar_б = 25$); ***2***, ***5*** – только донная продувка ($Ar_д = 25$)

and shows V_i, V_{av} values for each velocity vector at the corresponding coordinate point.

As it follows from the data in Fig. 4, the geometry of the streamlines and the value of the liquid circulation velocity depend on the blowing conditions and the coordinates of the flow points in the bath. A vortex zone 22.0 mm wide and 37.9 mm high, being limited by the extreme values of *x* (79.9—101.9 mm) and *y* (80.6—118.5 mm) and remote from the inner surface of the reactor shell at a distance of 27 mm (curve *5*) is formed near the liquid surface and the shell. At this point, the instantaneous velocity of the liquid flow element varies from 69.9 to 183.1 mm/s with an average velocity of 123.8 mm/s. The circulation flows fade in the bulk of liquid, resulting in V_{av} decreasing from 123.8 (curve *5*) to 47.0 and 54.1 mm/s (curves *6* and *7*, respectively). The difference in velocities can be explained by the wave nature of the oscillations of the gas-liquid system on the surface due to the factors of hydrodynamic instability of the bulk of liquid due to the pulsating mode of gas outflow [1, 2]. Approaching the reaction zone to the blowing jet results in increasing V_i values from 70.2 to 81.9 mm/s (curves *4*, *8*) and, on the contrary, decreasing them from 76.4 to 30.2 as well as from 46.3 to 26.2 mm/s (curves *7* and *6*). A further increase in velocity to 42.6 and 83.4 mm/s occurs due to the displacement of the flow towards the surface of the reactor shell, which also constitutes the reason for motion trajectory changes (curves *5*—*7*).

Blowing area *A*, where the lateral and bottom jets produce a combined impact on the liquid, is of particular interest. The comparison of V_i values for comparable coordinates in *A* and *B* areas reveals a higher circulation velocity under the combined impact of the jets on the liquid, for instance, 86.0 mm/s (curve *1*) and 81.9 mm/s (curve *8*). Curve *1* is shown more precisely in Fig. 2, from which it can be seen that upon approaching the zone of impact of the lateral stream, the direction of the flow changes at the point with (–42.0; 55.7 mm) coordinates (the dashed line indicates a hypothetically possible continuation of the motion trajectory), the instantaneous velocity increases from 9.5 to 15.9 mm/s (see Fig. 4). Note that even at a lower blowing intensity (curve *3*), V_i and V_{av} values are 105.8 and 92.9 mm/s, which is significantly higher than similar values in most areas of the considered velocity field. In the liquid circulation zone created only by the lateral jet (curve *3a*), value V_{av} = 77.4 mm/s appears to be higher than the corresponding value of 54.1 mm/s (curve *7*) in the bottom stream area. Upon that, the instantaneous velocity developed by the liquid at the same distance from the reactor shell is 91.4 mm/s at the lateral blowing and it is 30.2 mm/s near the bottom jet. This can be explained by additional swirling of the liquid flow in the near-wall area due to the introduction of the blowing at an angle of swinging to horizontal axis (Fig. 1).

The scheme of liquid flows at higher values of Archimedes criterion is shown in Fig. 5, from which it follows that the previously revealed regularities of liquid motion are generally retained. Upon that, the circulation velocity in the considered areas of the bath (*A*, *B*) increases, for instance, according to the data shown in Fig. 4, V_{av} value is 52.9 and 92.9 mm/s in area *A*, 47.0 and 54.1 mm/s in area *B*, whereas at high Ar values (Fig. 5) V_{av} increases up to 121.3 and 112.0 mm/s, respectively. Upon comparing the trajectories of motion of liquid elements (curves *2* and *3* in Fig. 5), it can be seen that at comparable coordinates of points (–43.3; 72.3 and 42.2; 78.5) V_i value is higher for the area of the combined impact of the streams (153.4 mm/s) than in the vicinity of the bottom jet (90.9 mm/s).

The intensity of circulation motions in the liquid is related to the energy impact of the streams on the corresponding areas of the liquid and is determined by Archimedes dynamic criterion at the nozzle outlet [12]. Therefore, the circulation velocity increases upon an increase in Ar value, which is particularly noticeable in the overlapping area of lateral and bottom streams (area *A*). The geometric dimensions of this zone depend on the range of the lateral jet and the width of the bottom

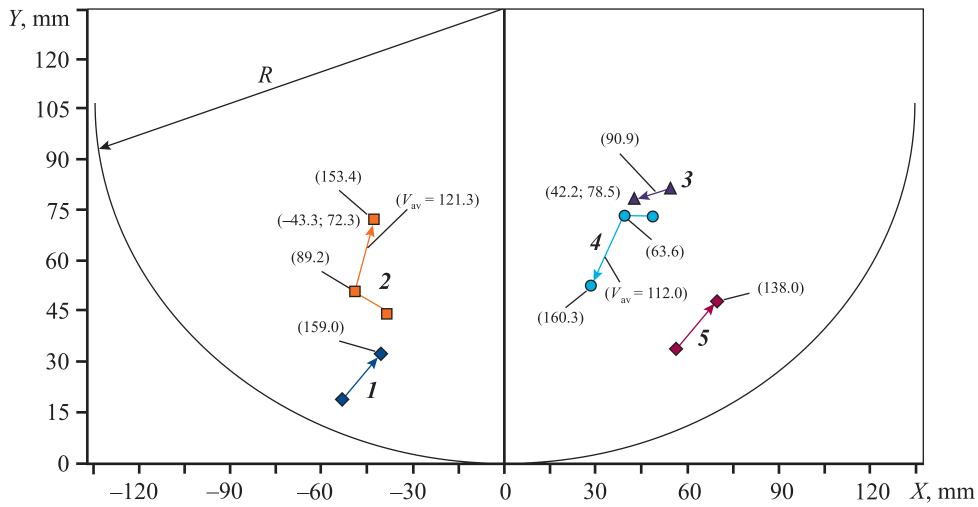

Fig. 5. Streamlines and the field of liquid motion velocities depending on Ar criterion
1, ***4***, ***5*** – $Ar_l = Ar_b = 60$; ***2***, ***3*** – $Ar_l = 120$; $Ar_b = 60$

Рис. 5. Линии тока и поле скоростей движения жидкости в зависимости от критерия Ar
1, ***4***, ***5*** – $Ar_б = Ar_д = 60$; ***2***, ***3*** – $Ar_б = 120$; $Ar_д = 60$

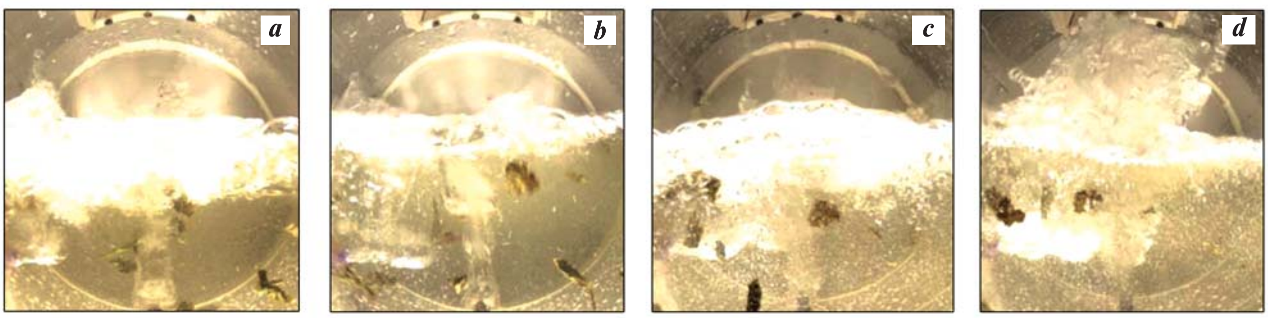

Fig. 6. The film fragments of the reaction zone depending on the size of the jet and Archimedes criterion upon reaching the extreme limits of the lateral stream range
a, ***b*** – $Ar_l = Ar_b = 60$; ***c***, ***d*** – $Ar_l = 120$; $Ar_b = 60$
a, ***c*** – minimum lateral stream range; ***b***, ***d*** – the maximum one

Рис. 6. Кинофрагменты реакционной зоны в зависимости от размеров факела и критерия Архимеда при достижении экстремальных границ дальнобойности боковой струи
a, ***b*** – $Ar_б = Ar_д = 60$; ***c***, ***d*** – $Ar_б = 120$; $Ar_д = 60$
a, ***c*** – минимальная дальнобойность боковой струи; ***b***, ***d*** – максимальная

jet, which are constantly changing due to the pulsation of the streams.

Fig. 6 shows the fragments of the reaction zone between the lateral and bottom jets at the moment of reaching the minimum (*a*, *c*) and the maximum (*b*, *d*) range of the lateral stream. It can be seen from the image in Fig. 6 (*d*) that with the relative constancy of the geometrical dimensions of the bottom stream due to Ar_b = const, the lateral jet under the conditions of $Ar_l = 120$ is in contact with the bottom stream. Upon less intensive blowing, a liquid area, being free from the interaction of streams, is observed (Fig. 6, *b*) between the lateral and bottom streams. The comparison of film fragments (Fig. 6, *b* and *d*) also exhibits that the direct contact of the blowing jets and the merging of their gas volumes are simultaneously accompanied by increased spatter formation. Furthermore, a high value of the Ar_b criterion and, accordingly, the length of the bottom stream can cause the formation of a “breakdown” of the bath [2], which results in a decrease in the degree of blowing oxygen uptake and an increase in the removal of the melt with spatter. According to the blowing macropattern (Fig. 6, *d*), such a mode is possible at $Ar_b = 60$, $Ar_l = 120$, therefore, it is of interest to estimate the velocity of circulation flows for variable values of Ar_b and Ar_l.

The table presents the data on liquid motion velocities in different parts of the bath, linked to the coordinate system (Fig. 4, 5), depending on the values of Ar_b, Ar_l upon $Ar_b \neq Ar_l$.

As a result of the analysis of the data specified in the table, the closest coordinates of the points were identified and the corresponding values Ar_b, Ar_l, V_i, V_{av} were determined. Data classification was performed using “*k* means” algorithm [22] and “Scikit-learn” standard cluster library [23]. The lines that characterize the trajectory of the movement of a particular indicator are marked with a horizontal line in the table. This allows to estimate the average circulation velocity along the entire length of the streamline *S*. The minimum discrepancy between the coordinates of the points was found in lines *1*, *21*; *11*, *24*; *13*, *26*; *16*, *28*; *4*, *24*; *8*, *26*, where the velocity value is least dependent on the location of the flow and is determined by other factors. The comparison of the table data (lines *11*, *24*; *13*, *26*; *16*, *28*) reveals that an increase in the bottom blowing intensity at Ar_l = const reduces the liquid circulation velocity. An increase in Ar_l at Ar_b = const causes an increase in the instantaneous and average velocities (lines *1*, *21*). The explanation of the specified regularities is as follows: In the general case, the mixing of the bath is performed due to the force impact of circulation

Liquid circulation velocity upon blowing through the lateral and bottom nozzles depending on the location of the flow and Archimedes criteria

Скорость циркуляции жидкости при продувке через боковое и донное сопла в зависимости от местоположения потока и критериев Архимеда

Archimedes criterion		Coordinates, mm		Velocity, mm/s		Line
Ar_b	Ar_l	*X*	*Y*	V_i	V_{av}	
1	*2*	*3*	*4*	*5*	*6*	*7*
		–16.5	71.2	80.0	–	*1*
		–21.8	85.4	105.8	92.9	*2*
		–29.5	64.4	135.7	–	*3*
		–25.4	53.8	79.6	–	*4*
5	25	–25.1	25.8	195.6	137.0	*5*
		12.4	90.3	58.9	–	*6*
		15.2	83.9	48.3	–	*7*
		18.8	64.3	139.1	–	*8*
		17.4	34.2	210.2	114.1	*9*
		–37.8	43.5	82.0	–	*10*
		–30.9	37.0	66.1	–	*11*
		–22.1	37.0	63.0	70.4	*12*
		26.2	34.4	101.2	–	*13*
25	60	38.6	42.1	102.1	–	*14*
		45.0	46.5	55.1	86.1	*15*
		101.0	102.8	50.6	–	*16*
		93.8	80.6	163.0	–	*17*
		95.5	70.0	76.7	–	*18*
		107.9	78.2	104.2	98.6	*19*
		–21.3	61.1	88.1	–	*20*
		–14.4	54.9	64.8	76.4	*21*
		–59.9	35.9	4.31	–	*22*
		–45.5	29.0	111.2	–	*23*
		–28.7	29.5	117.6	77.7	*24*
5	60	29.3	59.8	60.3	–	*25*
		18.8	34.8	189.1	–	*26*
		29.5	31.7	78.1	109.2	*27*
		102.4	95.6	143.2	–	*28*
		88.0	99.6	104.0	–	*29*
		96.3	121.0	160.1	135.8	*30*

flows and turbulent pulsations on the liquid [6]. Thus, the observed liquid velocity (V_i, V_{av}) represents the sum of the circulation (V_c) and pulsation (V_p) components of the velocity. Therefore, the different impact of the lateral and bottom blowing can be caused by the occurrence of turbulent pulsations in the gas-liquid two-phase flow, the appearance of which causes oscillations of the bath.

The visualization results (Fig. 7, 8) attest to the fact that depending on Ar_b, Ar_l and the current blowing time, 3 main types of oscillations of the phase interface, i.e. gas-liquid and liquid layers of the bath, arise. The first one includes the vertical displacement of the horizontal plane of the main bulk of liquid by Δh_l value (Fig. 7 *a*, *b*). The oscillations of the 2nd type form a wave-like motion of the liquid near the surface of the bath (Fig. 7, *c*). In this case, Δh_l is defined as the difference between the average horizontal lines between the levels of the main bulks of pure liquid. The oscillations of the 3rd type (Fig. 8, *a*—*c*) are characterized by opposite angles of swinging of the phase interface to the horizontal axis (for instance, 5°, 8°). This type of oscillation causes boundary vertical displacements of the liquid of various sizes Δh_l on the inner surface of the reactor. All these 3 types of oscillation can be seen on a single film record.

To estimate the impact of each type of blowing on the overall macropattern of oscillations, the state of the liquid bath was considered under similar dynamic conditions of separate blowing for the lateral and bottom streams. Fig. 9 (*c*) shows the fragments of film record of liquid bubbling by single nozzles. As per Fig. 9 (*a*), it can be seen that wave-like oscillations of the 2nd type, being close to the sinus one with amplitude *A*, is

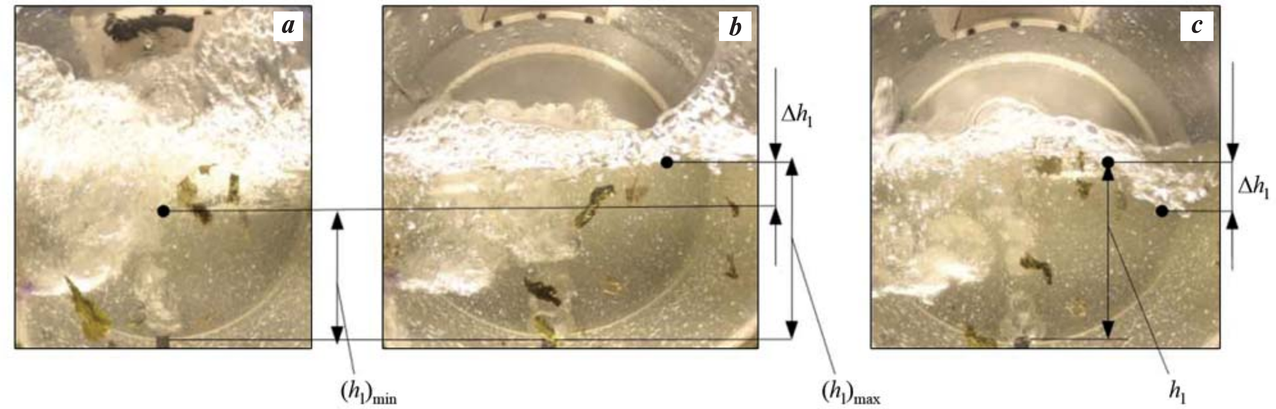

Fig. 7. Film fragments of transverse (***a***, ***b***) and wave-like (***c***) oscillations of the liquid at $Ar_l = 60$, $Ar_b = 5$
Δh_l – average change in the liquid level

Рис. 7. Кинофрагменты видов поперечного (***a***, ***b***) и волнообразного (***c***) колебаний жидкости при $Ar_б = 60$, $Ar_д = 5$
$\Delta h_ж$ – среднее изменение уровня жидкости

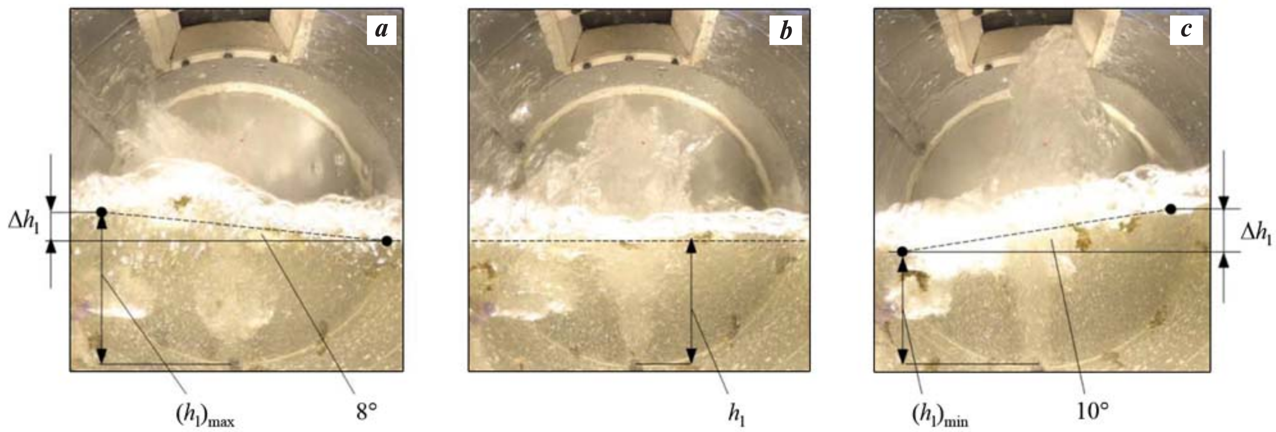

Fig. 8. The film fragments of successive changes in the averaged line of the interface between the gas-liquid and liquid layers of the bath depending on the current blowing time (τ_i) at $Ar_l = 60$, $Ar_b = 25$
τ_i, s: ***a*** – 0.143; ***b*** – 0.286; ***c*** – 0.429

Рис. 8. Кинофрагменты последовательного изменения усредненной линии границы раздела газожидкостного и жидкого слоев ванны в зависимости от текущего времени продувки (τ_i) при $Ar_б = 60$, $Ar_д = 25$
τ_i, с: ***a*** – 0,143; ***b*** – 0,286; ***c*** – 0,429

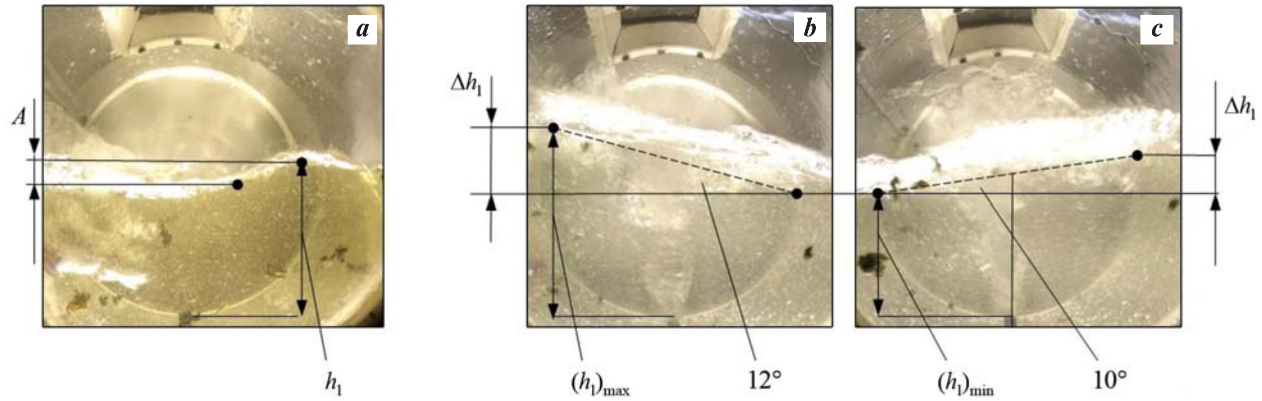

Fig. 9. The types of oscillations depending on the type of separate blowing at different values of Archimedes criterion
a – the lateral blowing, $Ar_l = 60$; ***b***, ***c*** – the bottom blowing, $Ar_b = 25$; the dashed line indicates the middle line of the phase boundary

Рис. 9. Разновидности колебаний в зависимости от вида отдельной продувки при различных значениях критерия Архимеда
a – боковая продувка, $Ar_б = 60$; ***b***, ***c*** – донная, $Ar_д = 25$; штрихом показана средняя линия границы раздела фаз

more clearly revealed when the lateral blowing is used. Stronger bath oscillation with the angles of 12° and 10° under the 3rd type occurs in the case of bottom blowing (Fig. 9, *b*, *c*). Therefore, upon combined blowing, the partial contribution of each type of blowing impacts the overall intensity and the type of oscillations of the liquid bath in a different way. The moderate introduction of the bottom blowing ($Ar_b = 5$) causes the wave-like motion of the liquid (Fig. 7, *c*) along with the oscillations of the 1st type (see Fig. 7, *a*, *b*), and at higher values $Ar_b = 25$, it causes angular oscillations (Fig. 8). Upon that, Δh_l value gradually decreases as the bubbling area approaches the geometric center of the reactor. In practice, this circumstance means that the mixing of the bath according to the 3rd type covers the volume of the melt near the center of the PMU to a lesser extent, and is mainly concentrated on the periphery near the lining of the unit. This can cause additional erosive wear of the lining in the area of lances. The wavy oscillations of the 2nd type are characterized by less oscillation amplitude and Δh_l value, therefore, in the near-wall zone they can exhibit a lesser impact on the lining. The mixing of the melt in the surface layer due to any oscillations contributes to the dissolution and adoption of charging material by the liquid bath of the unit. A further increase of the blowing intensity only by a bottom lance increases the liquid swing angles up to 18—15° (Fig. 10). The combined blowing reduces the intensity and changes the pattern of angular oscillations of the liquid due to the lateral jet, reducing the angles of swinging from 18—15° down to 8—10° (Fig. 9, *b*, *c*; Fig. 10; Fig. 8, *a*, *c*). In industrial conditions, this type of oscillations can cause additional erosion of the PMU lining.

The impact of phase interface oscillations on the liquid circulation velocity at various points of the reaction zone and under various blowing conditions was studied. The value of oscillations was estimated as difference between maximum and minimum height of the liquid: $\Delta h_l = (h_l)_{max} - (h_l)_{min}$ for full-wave oscillations (τ_i). The place of control of extreme values of the height of pure liquid (h_l) at the current time τ_i was determined visually, based on the minimum gas injections. In the presence of oscillations of the 1st type, h_l was taken as the value corresponding to the horizontal line of the liquid (Fig. 7, *a*, *b*; Fig. 8, *b*), in the presence of oscillations of the 2nd type — at the wave amplitude point (Fig. 7, *c*; Fig. 9, *a*), and in the presence of oscillations of the 3rd type — near the reactor wall, at the point of extremum (Fig. 8, *a*, *c*; Fig. 9, *b*, *c*).

Fig. 11 presents the results of estimation of h_l values at the boundary with the gas-liquid layer depending on

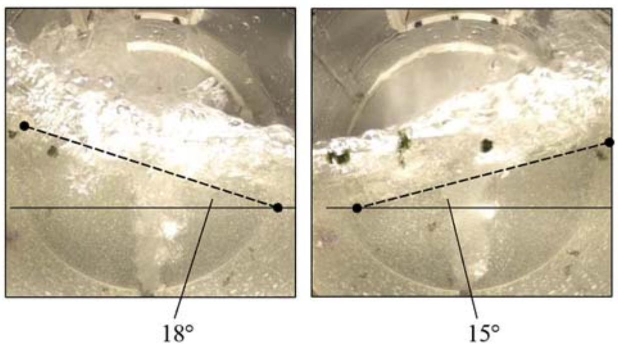

Fig. 10. The film fragments when the liquid is blown by the bottom lance at $Ar_b = 60$

Рис. 10. Фрагменты кинограммы при продувке жидкости донной фурмой при $Ar_д = 60$

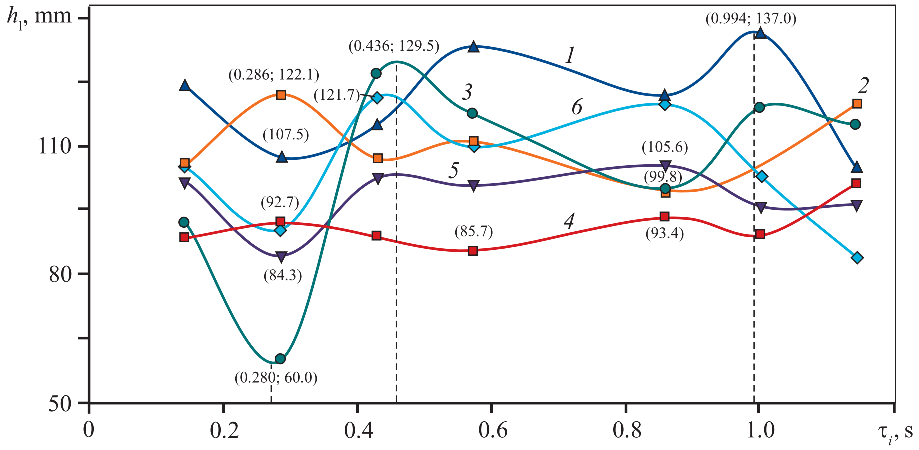

Fig. 11. The height of the liquid layer depending on the current time of the combined blowing and Archimedes criterion
1 – $Ar_l = 60$, $Ar_b = 5$; ***2*** – $Ar_l = Ar_b = 25$; ***3*** – $Ar_l = 120$, $Ar_b = 60$; ***4*** – $Ar_l = 25$, $Ar_b = 5$; ***5*** – $Ar_l = 60$, $Ar_b = 25$; ***6*** – $Ar_l = Ar_b = 60$

Рис. 11. Высота слоя жидкости в зависимости от текущего времени комбинированной продувки и критерия Архимеда
1 – $Ar_б = 60$, $Ar_д = 5$; ***2*** – $Ar_б = Ar_д = 25$; ***3*** – $Ar_б = 120$, $Ar_д = 60$; ***4*** – $Ar_б = 25$, $Ar_д = 5$; ***5*** – $Ar_б = 60$, $Ar_д = 25$; ***6*** – $Ar_б = Ar_д = 60$

the Archimedes criteria and the current blowing time τ_i. The coordinates of the extremum points of curves *1*, *3* are determined based on the approximation functions. The type of curves in Fig. 11 demonstrates that the surface oscillations are complex in nature with different extreme values of h_l and the values of the time to reach them.

The results of mathematical processing of the data from Fig. 11 (curves *3*, *4*) attest to the fact that the change in the surface level of the liquid bath (Δh_l) makes up 7.7—69.5 mm and depends on Archimedes criteria of the lateral and bottom blowing. Increasing the overall intensity of the combined blowing at $Ar_l = Ar_b$ results in the increase of Δh_l from 21.3 to 29.0 mm (Fig. 11, curve *2*, *6*). For these conditions, as previously noted, the value of the average liquid circulation velocity increases. The change of Δh_l from 21.3 to 29.5 mm (Fig. 11, curves *5* and *1*) for $Ar_b = 25$ and 5 increases V_i value from 66.1 to 117.6 mm/s (see the table, lines *11* and *24*) and V_{av} value from 70.4 to 77.7 mm/s (see the table, lines *12* and *24*) in area *A*. In area *B*, V_i value also increases from 50.6 to 143.2 mm/s (see the table, lines *16* and *28*), and V_{av} increases from 98.6 to 135.8 mm/s (see the table, lines *19* and *30*) under these conditions. The change of Ar_l from 25 to 60 ($Ar_b = 5 = const$) increases Δh_l value from 7.7 to 29.5 mm (Fig. 11, curves *4* and *1*). Upon that, V_i for area *A* increases from 79.6 to 88.1 mm/s (see the table, lines *4* and *20*). In the zone of interaction of the bottom stream only (*B*), V_{av} value also increases from 104.2 to 114.1 mm/s (see the table, lines *19* and *9*). Thus, the liquid circulation velocity is interconnected with the pulsating component of the flow motion and increases with an increase in the amplitude of oscillations at the phase boundary.

Conclusion

Over the range of $Ar_l = 12 \div 120$, $Ar_b = 5 \div 60$ values, cold modeling of the hydrodynamics of the bubbling PMU bath was performed with the combined blowing of the liquid by the lateral and bottom lances. A quantitative estimation of the velocity of liquid bath circulation, depending on the Archimedes criteria and the location of the flow, was performed. Three types of oscillations (pulsations) of the phase boundary "pure liquid — gas-liquid layer" were revealed. The analysis of the occurrence of each type of pulsation under various blowing conditions was performed. It is shown that the liquid circulation velocity depends on the intensity of oscillations, defined as the difference (Δh_l) between the maximum and minimum height of the pure liquid for full-wave oscillations. With regard to the stability of the PMU lining, the intensity of mixing of the near-surface layer and the adoption of charging material by the bath, the impact of each type of oscillations on the liquid circulation velocity was considered.

References

1. Bulatov K.V., Zhukov V.P, Bratygin E.V., Tomilov N.A., Menshikov V.A. Investigation of Pobeda furnace bubbling zone physics using cold modeling method. Part 1. Investigation of fluid and gas dynamics of bubbling using a side-blowing gas-protected lance. *Izvestiya. Non-Ferrous Metallurgy*. 2021; 27 (3): 15–23. (In Russ.).

Булатов К.В., Жуков В.П., Братыгин Е.В., Томилов Н.А., Меньщиков В.А. Исследование физических явлений в барботажной зоне плавильного агрегата «Победа» методом холодного моделирования. Сообщение 1. Исследование гидрогазодинамических закономерностей продувки жидкости газом с помощью боковой фурмы в защитной газовой оболочке. *Известия вузов. Цветная металлургия*. 2021; 27 (3): 15—23.

2. Bulatov K.V., Zhukov V.P., Bratygin E.V., Tomilov N.A., Menshikov V.A. Investigation of Pobeda furnace bubbling zone physics using cold modelling method. Part 2. Hydro-gas dynamics of liquid blowing with gas using bottom gas-protected lance. *Izvestiya. Non-Ferrous Metallurgy*. 2022; 28 (1): 4—14. (In Russ.).
Булатов К.В., Жуков В.П., Братыгин Е.В., Томилов Н.А., Меньщиков В.А. Исследование физических явлений в барботажной зоне плавильного агрегата «Победа» методом холодного моделирования. Сообщение 2. Гидрогазодинамика продувки жидкости газом с помощью донной фурмы в защитной газовой оболочке. *Известия вузов. Цветная металлургия*. 2022; 28 (1): 4—14.
3. Bulatov K.V., Zhukov V.P., Bratygin E.V., TomilovN.A., Menshikov V.A. Investigation of Pobeda furnace bubbling zone physics using cold modelling method. Part 2. Hydro-gas dynamics of liquid blowing by gas using bottom gas-protected lance. *Russian Journal of Non-Ferrous Metals*. 2022; 63 (2): 113—120.
4. Nakanishi K., Fujii T., Szekely J. Possible relationship between energy dissipation and agitation in steel-processing operations. *Ironmaking & Steelmaking*. 1975; 2 (3): 193—197.
5. Bulatov K.V., Yakornov S.A., Ibragimov A.F., Iskhakov I.I. Industrial tests of sulphide copper concentrate melting in smelter Pobeda on oxygen blow using botton tuyeres. *Metallurgist*. 2020; (8): 36—40. (In Russ.).
Булатов К.В., Якорнов С.А., Ибрагимов А.Ф., Исхаков И.И. Промышленные испытания плавки сульфидного концентрата в ПАП на кислородном дутье с использованием донных фурм. *Металлург*. 2020; (8): 36—40.
6. Surin V.A., Nazarov Yu.N. Mass and heat transfer, hydrogas dynamics of a metallurgical bath. Moscow: Metallurgiya, 1993. (In Russ.).
Сурин В.А., Назаров Ю.Н. Массо- и теплообмен, гидрогазодинамика металлургической ванны. М.: Металлургия, 1993.
7. Dyudkin D.A., Kisilenko V.V. Modern steel production technology. Moscow: Teplotekhnika, 2007. (In Russ.).
Дюдкин Д.А., Кисиленко В.В. Современная технология производства стали. М.: Теплотехника, 2007.
8. Fluid Flow, Duan Zhang, Lifeng Thomas, Brian Conejo. Dissolution, and mixing phenomena in argon-stirred steel ladles. *Metallurgical and Materials Transactions B*. 2018; 49: 2722—2743.
9. Gajjar Prince, Haas T.N., Kwaku Boateng Owusu, Moritz Eickhoff, Pruet Kowitwarangkul, Herbert Pfeifer. Physical study of the impact of injector design on mixing, convection and turbulence in ladle metallurgy. *Engineering Science and Technology*. 2019; 22: 538—547.
10. Rogotovskii A.N., Shipelnikov A.A., Bobyleva N.A., Rogotovskii A.N. Modeling of the melt movement in the tundish of a continuous casting machine with the presence of flow modifiers. *Lipetsk State Technical University*. 2018; 37 (3): 87—94. (In Russ.).
Роготовский А.Н., Шипельников А.А., Бобылева Н.А., Роготовский В.Н. Моделирование движения расплава в промежуточном ковше машины непрерывного литья заготовок с различными модификаторами потока. *Вестник Липецкого государственного технологического университета*. 2018; 37 (3): 87—94.
11. Panteikov S.P. Technology of combined bottom blowing with oxygen and inactive gases in converters. *Ferrous Metallurgy. Bulletin of Scientific, Technical and Economic Information*. 2017; (7): 55—67. (In Russ.).
Пантейков С.П. Технология комбинированной продувки кислородом сверху и неактивными газами через днище в конвертерах. *Черная металлургия. Бюллетень научно-технической и экономической информации*. 2017; (7): 55—67.
12. Chernatevich A.G, Molchanov L.S., Sigarev E.N., Dudchenko S.A., Vakul'chuk V.V., Yushkevich P.O., Chubin K.I., Pokhvalityi A.A., Chubina E.A. Video recording of physical and chemical processes in the converter cavity during the top blowing of the bath using various designs of oxygen lances. Part 1. Installations and methodology for conducting research. *Ferrous Metallurgy. Bulletin of Scientific, Technical and Economic Information*. 2021; 77 (8): 969—976. (In Russ.).
Чернатевич А.Г., Молчанов Л.С., Сигарев Е.Н., Дудченко С.А., Вакульчук В.В., Юшкевич П.О., Чубин К.И., Похвалитый А.А., Чубина Е.А. Видеофиксация физико-химических процессов в полости конвертера при верхней продувке ванны с использованием различных конструкций кислородных фурм. Сообщение 1. Установки и методика проведения исследований. *Черная металлургия. Бюллетень научно-технической и экономической информации*. 2021; 77 (8): 969—976.
13. Chernyatevich A.G., Sigarev E.N., Molchanov L.S. A picture of blowing a converter bath using a two-tier oxygen

lance. *Ferrous Metallurgy. Bulletin of Scientific, Technical and Economic Information*. 2017; (12): 39–45. (In Russ.).
Чернятевич А.Г., Сигарев Е.Н., Молчанов Л.С. Картина продувки конвертерной ванны с использованием двухъярусной кислородной фурмы. *Черная металлургия. Бюллетень научно-технической и экономической информации*. 2017; (12): 39–45.
14. Jiang X., Cui Z., Chen M., Zhao B. Mixing behaviors in the horizontal bath smelting furnaces. *Metallurgical and Materials Transactions B*. 2019; 50 (1): 173–180.
15. Jiang X., Cui Z., Chen M., Zhao B. Study of plume eye in the copper bottom-blown smelting furnace. *Metallurgical and Materials Transactions B*. 2019; 50: 765–778. https://doi.org/10.1007/s11663-019-01516-0
16. Shijie Wang, William Davenport. Coppersmelting: world copper smelter data. *Copper*. 2016; 3: 29–31.
17. Liam J., Joel P.T. The 2019 copper smelting survey. In: *Pyrometallurgy. Smeltihg operation: Proceedings Copper 2019 – Cobre International Conference* (Montreal, Quebec, Canada). 2019; 4 (1): 10.
18. Matusevic R.W., Baldock B.R., Robert J.S. Ausmelt technology recycling of computer board and other high value materials. In: *European Metallurgical Conference EMC* (Friedrichshafen, Germany). 2001; 2: 151–163.
19. Baldock B.R., Short W.E. Australian technology on the world scene. Update on Ausmelt plants and projekts. In: *MINREX 2000: International Congress on mineral processing and extractive metallurgy* (Melbourne, Australia). 2000. P. 164–169.
20. Yusupkhodjaev A.A., Matharimov S.T., Nosirhodjaev S.K. Wirkungen Technologien in der Kupferpyrometallurgien. `Deutschland: Lambert Academic Publishing, 2019.
21. Yusupkhodjaev A.A., Khojiev S.T., Berdyarov D.O. Technology of processing slags of copper production using local secondary technogenic formations. *International Journal of Innovative Technology and Exploring Engineering*. 2019; 9 (1): 5461–5472. https://doi.org/10.35940/ijitee. A4851119119.119119
22. MacQueen J. Some methods for classification and analysis of multivariate observations. In: *Proceedings 5th Berkeley Symposium on mathematical statistics and probability*. 1967; 281–297.
23. Mueller A., Guido S. Introduction to machine learning with Python: A guide for data scientists. Sebastopol, USA: Publ. by O'Reilly Media, Inc., 2016.
Мюллер А., Гвидо С. Введение в машинное обучение с помощью Python: Рук-во для специалистов по работе с данными. М.: O'Reilly, 2017.

Information about the authors

Konstantin V. Bulatov – Cand. Sci. (Eng.), General Director of the JSC "Ural Research and Design Institute of Mining Processing, Metallurgy, Chemistry, Standartization" (JSC "Uralmekhanobr").
https://orcid.org/0000-0001-8474-598X
E-mail: Bulatov_KV@umbr.ru

Vladimir P. Zhukov – Dr. Sci. (Eng.), Prof., Leading Researcher of the Laboratory of Sintering and Physical and Mechanical Tests (LSPMT), JSC "Uralmekhanobr".
https://orcid.org/0000-0002-3030-0077
E-mail: zhukov.v.p@mail.ru

Evgenii V. Bratygin – Cand. Sci. (Eng.), Chief of Laboratory LSPMT, JSC "Uralmekhanobr".
https://orcid.org/0000-0003-4049-3797
E-mail: bev@umbr.ru

Nikolay A. Tomilov – Engineer of Laboratory LSPMT, JSC "Uralmekhanobr".
https://orcid.org/0000-0002-2869-2892
E-mail: tomilov.n@yahoo.com

Vikentii A. Menshchikov – Cand. Sci. (Eng.), Engineer of the Department of Non-Ferrous Metallurgy, Ural Federal University n.a. the First President B.N. Eltsin.
https://orcid.org/0000-0002-5474-8829
E-mail: kvadron@yandex.ru

Информация об авторах

Константин Валерьевич Булатов – к.т.н., генеральный директор ОАО «Уральский научно-исследовательский и проектный институт горного дела, обогащения, металлургии, химии, стандартизации» (ОАО «Уралмеханобр»).
https://orcid.org/0000-0001-8474-598X
E-mail: Bulatov_KV@umbr.ru

Владимир Петрович Жуков – д.т.н., профессор, ведущий научный сотрудник лаборатории окускования и физико-механических испытаний (ОиФМИ), ОАО «Уралмеханобр».
https://orcid.org/0000-0002-3030-0077
E-mail: zhukov.v.p@mail.ru

Евгений Владимирович Братыгин – к.т.н., заведующий лабораторией ОиФМИ, ОАО «Уралмеханобр».
https://orcid.org/0000-0003-4049-3797
E-mail: bev@umbr.ru

Николай Алексеевич Томилов – инженер лаборатории ОиФМИ, ОАО «Уралмеханобр».
https://orcid.org/0000-0002-2869-2892
E-mail: tomilov.n@yahoo.com

Викентий Алексеевич Меньщиков – к.т.н., инженер кафедры металлургии цветных металлов, Уральский федеральный университет им. первого Президента России Б.Н. Ельцина.
https://orcid.org/0000-0002-5474-8829
E-mail: kvadron@yandex.ru

Contribution of the authors

K.V. Bulatov – formation of the main concept, setting the goal and objectives of the study, preparation of the text, formulation of conclusions.

V.P. Zhukov – scientific guidance, analysis of research results, correction of the text of the article.

E.V. Bratygin – development of a methodology for processing experimental data, management of the experiment, resources supply.

N.A. Tomilov – processing of experimental data, performing calculations.

V.A. Menshchikov – the experimental technique substantiation, processing of research results.

Вклад авторов

К.В. Булатов – формирование основной концепции, постановка цели и задачи исследования, подготовка текста, формулировка выводов.

В.П. Жуков – научное руководство, анализ результатов исследований, корректировка текста статьи.

Е.В. Братыгин – разработка методологии обработки экспериментальных данных, руководство проведением эксперимента, обеспечение ресурсами.

Н.А. Томилин – обработка экспериментальных данных, выполнение расчетов.

В.А. Меньщиков –обоснование техники эксперимента, обработка результатов исследований.

The article was submitted 05.09.2022, accepted for publication 11.10.2022

Статья поступила в редакцию 05.09.2022, подписана в печать 11.10.2022